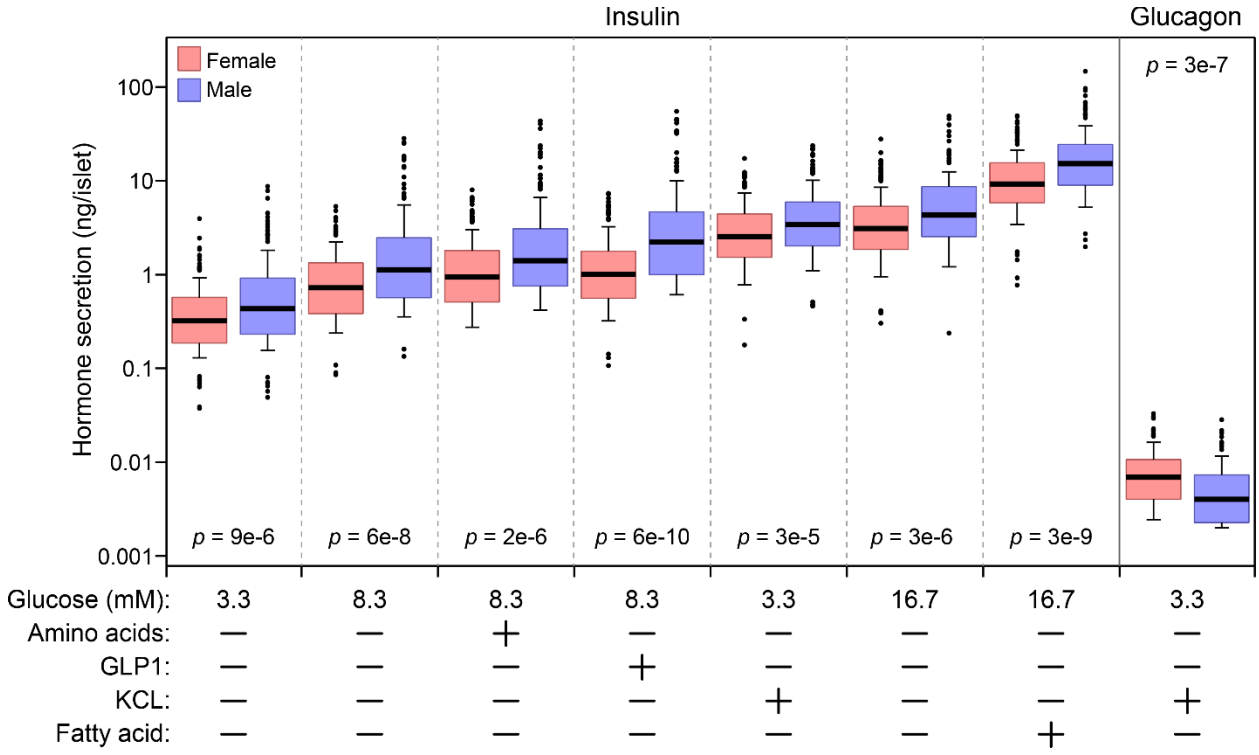

Figure S1. Insulin and glucagon secretion from pancreatic islets show a strong sex difference.
Ex vivo insulin and glucagon secretion are shown for 7 different secretagogue conditions in islets from female and male DO mice maintained on the HF/HS diet. Amino acids; leucine (0.5 mM), alanine (1.25 mM), and glutamine (2 mM). KCl (40 mM); GLP1 (100 nM); and fatty acid (palmitate, 0.5 mM). Insulin secretion values are the geometric means of 6 individual measures/condition/mouse for 479 DO mice, for a total of ~20,000 measurements. KCl-induced glucagon secretion was determined from a single measurement from 178 female, and 187 male DO mice. P-values for sex differences are shown for each phenotype (Student's 2-tailed t-test).

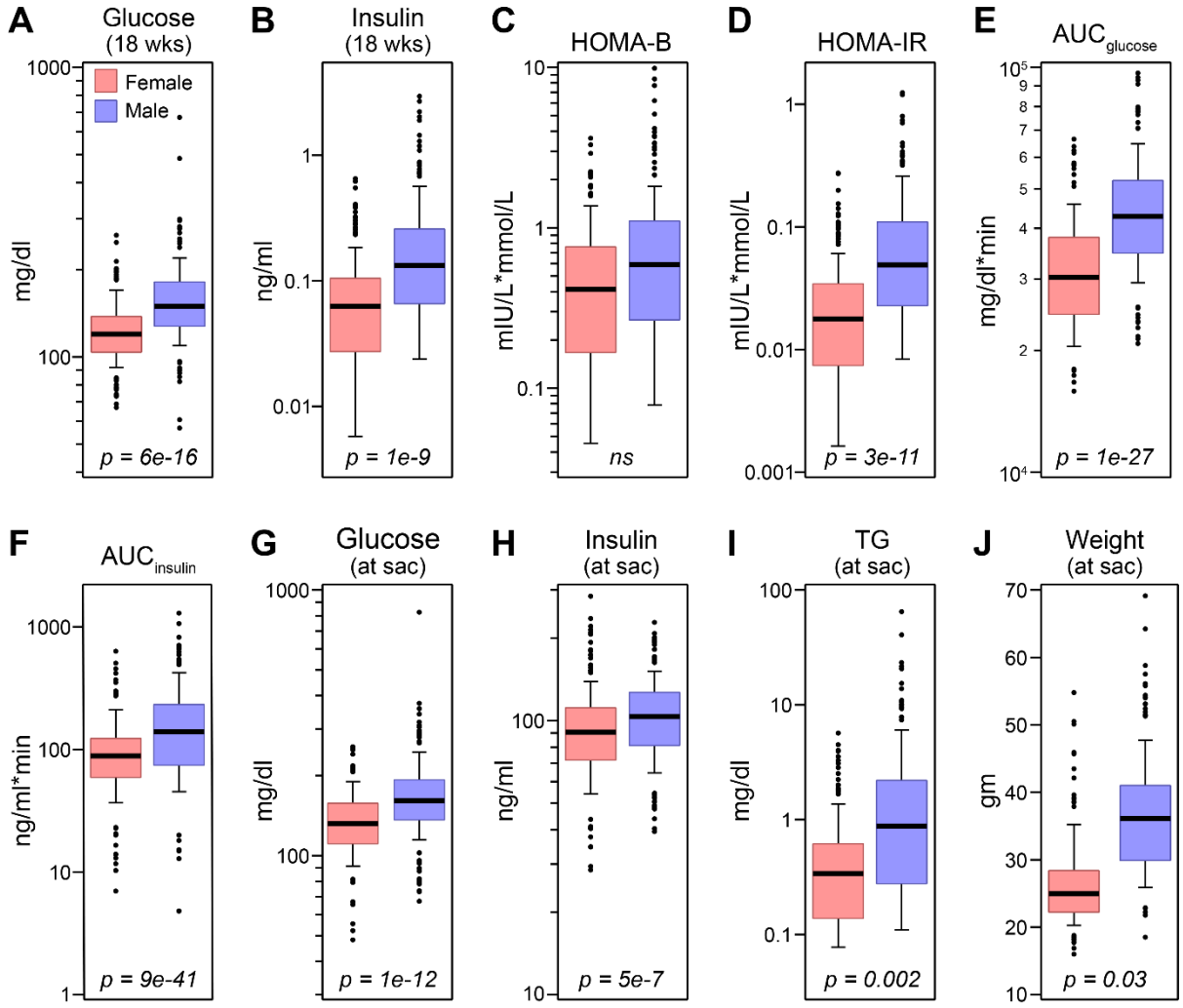

Figure S2. Metabolic phenotypes show a broad range and are influenced by sex.
Fasting plasma glucose (**A**) and insulin (**B**), HOMA-B (**C**), HOMA-IR (**D**), AUC values from an oGTT for glucose (**E**) and insulin (**F**), and measures at sacrifice for plasma glucose (**G**), insulin (**H**), triglycerides (TG, **I**) and body weight (**J**) are shown for female (240) and male (243) DO mice. P-values indicate significance for a sex difference for each phenotype (Student's 2-tailed t-test); *ns*, not significant. HOMA metrics were computed from glucose and insulin values determined at 18 weeks of age. AUC determinations were made from oGTT performed at 18 weeks. Sac; sacrifice.

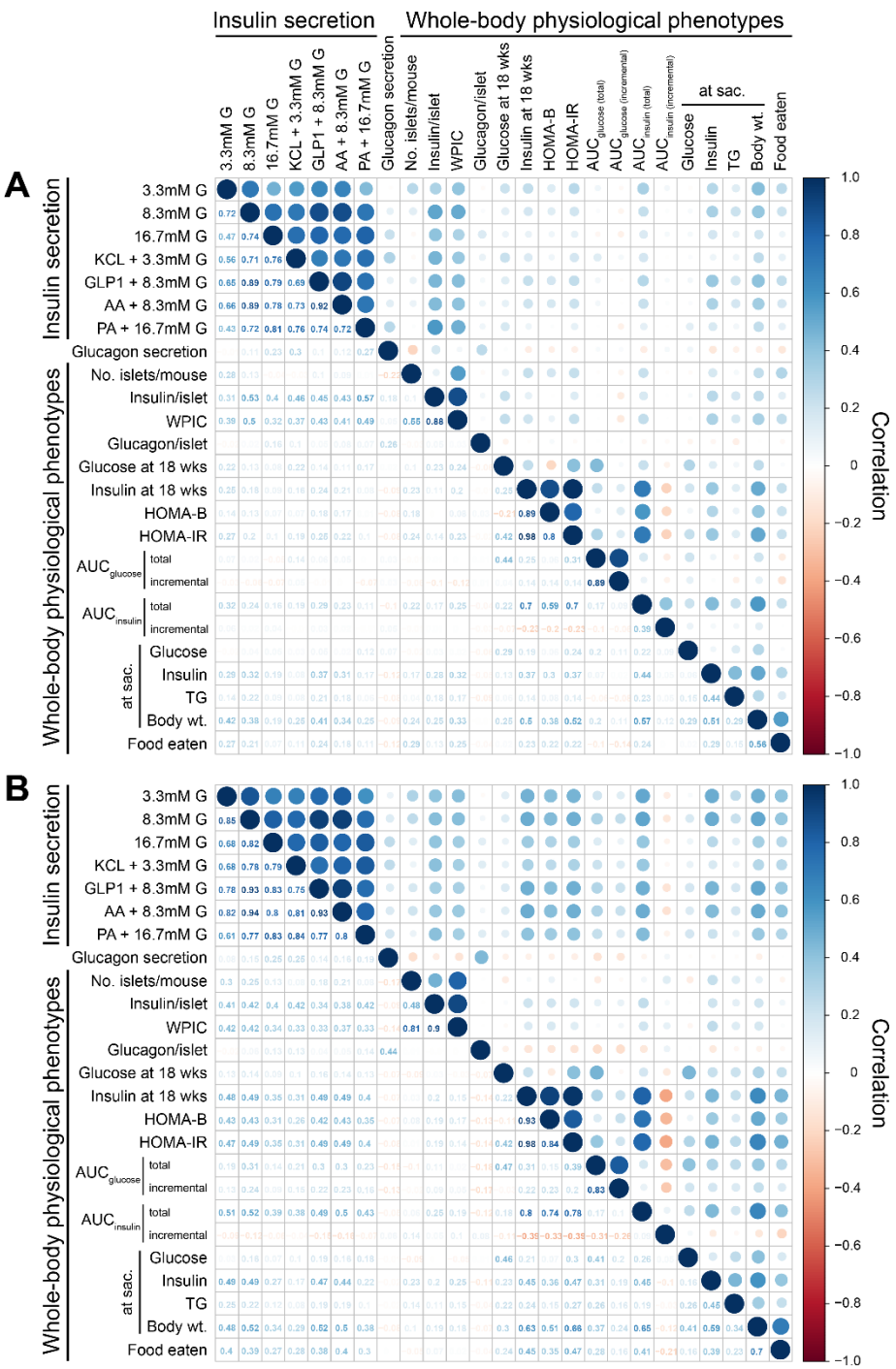

Figure S3. Correlation structure of secretion and whole-body physiological traits among DO mice.

The pair-wise Pearson's correlations between all secretion traits (insulin and glucagon) and physiological traits measured in female (**A**) and male (**B**) DO mice maintained on the HF/HS diet. All traits were log-transformed prior to computing the correlations. Color scale shows positive (blue) versus negative (red) correlations. Color intensity and diameter of circles in right triangle represents correlations graphically, while the correlation values for each comparison are shown in the left triangle. Data derive from analysis of 479 DO mice.

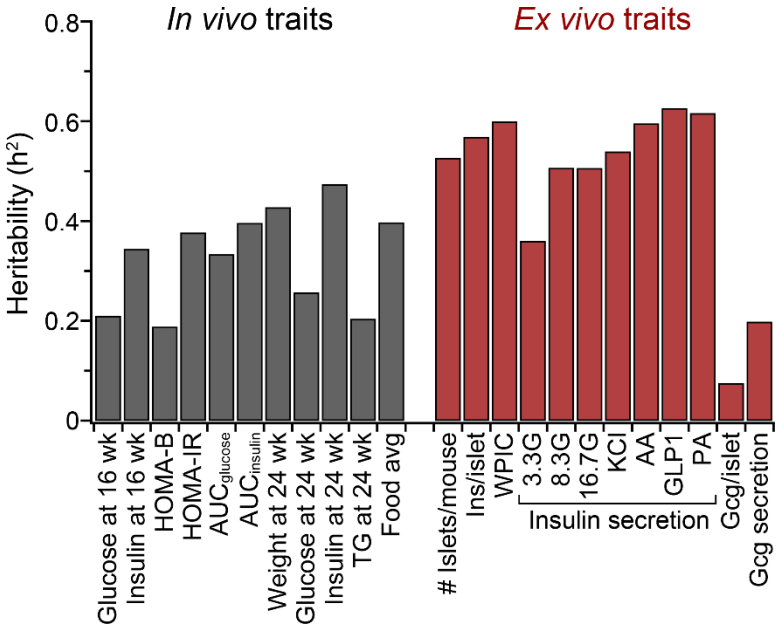

Figure S4. Heritability estimates for phenotypes measured in DO mice.
Heritability was computed for whole-body physiological phenotypes (*In vivo* traits), and for phenotypes measured from cultured islets (*Ex vivo* traits) harvested from 479 DO mice.

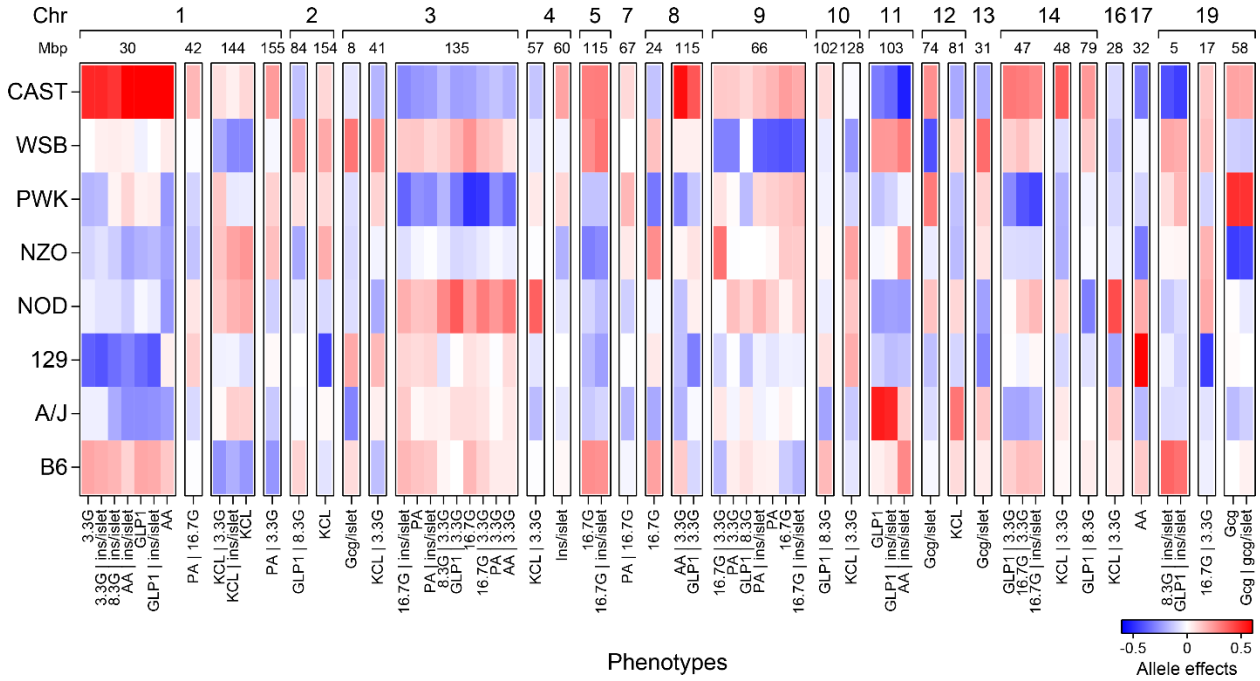

Figure S5. Allele effect patterns at secretion QTL hotspots.
Allele effect values for individual QTL (LOD > 6) are illustrated for *ex vivo* insulin and glucagon secretion, and the whole-islet contents for insulin (Ins/islet) and glucagon (Gcg/islet). Secretion traits were either mapped as straight secretion, or after conditioning (|) on glucose concentration (3.3, 8.3 or 16.7 mM), Ins/islet or Gcg/islet. Glucagon secretion in response to KCl + 3.3 mM glucose is listed as "Gcg", whereas all other secretion traits are for insulin secretion in response to the condition listed. At loci where more than one trait co-mapped, common allele effect patterns were used to define one QTL; e.g., Chr 1 at 30 Mbp. At these QTL, the average genomic position (Mbp) for QTL peak of the individual traits is shown. Data derive from QTL analysis of 479 DO mice.

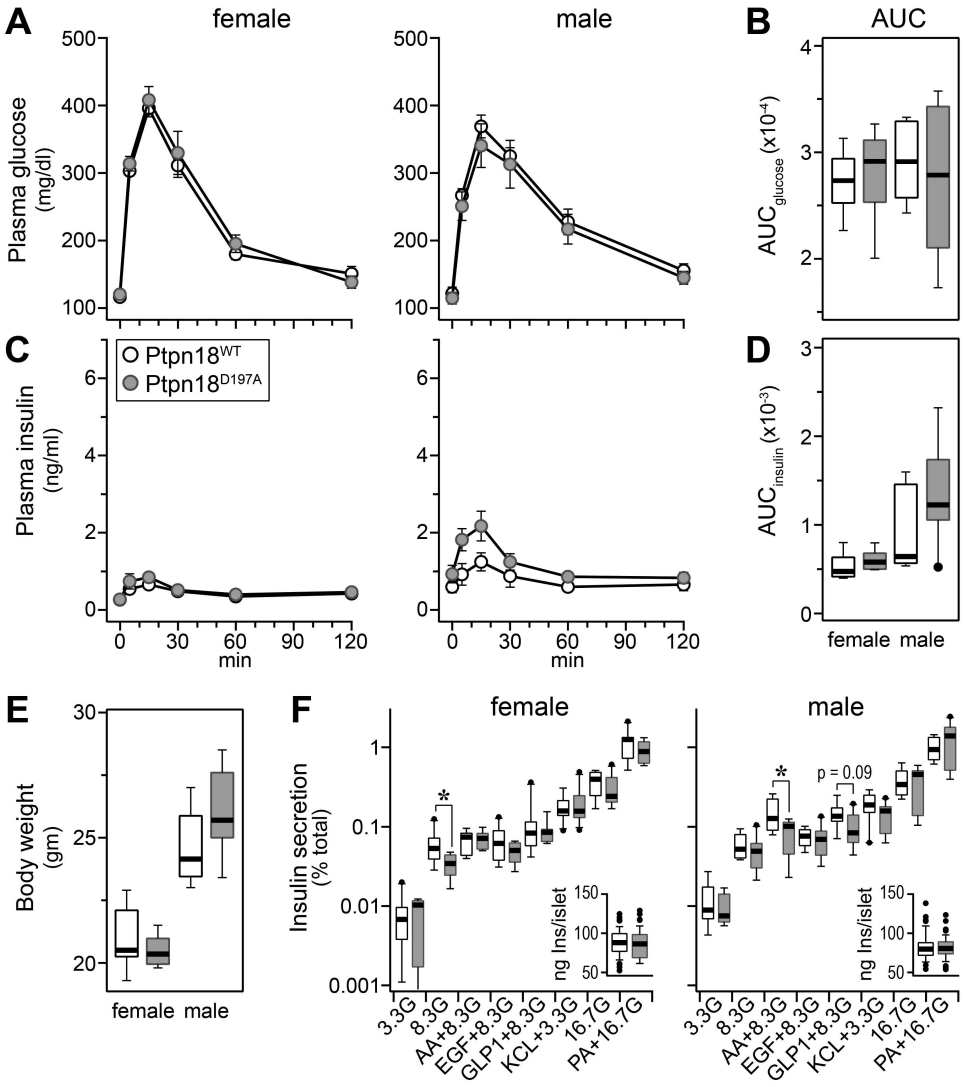

Figure S6. Glucose tolerance and insulin secretion in chow-fed *Ptpn18^{D197A}* mice. Plasma glucose (**A**) and insulin (**C**) during an oGTT in female (n=9, 6) and male (n=6, 9) wild type (*Ptpn18^{WT}*) and *Ptpn18^{D197A}* mice, respectively; area under the curve (AUC) for glucose (**B**) and insulin (**D**). Body weight at 10 weeks of age in female (n=9, 6) and male (n=6, 9) *Ptpn18^{WT}* and *Ptpn18^{D197A}* mice, respectively (**E**). *Ex vivo* insulin secretion measurements in female (n=10, 11) and male (n=8, 10) *Ptpn18^{WT}* and *Ptpn18^{D197A}* mice, respectively. Insets, whole islet insulin content. *, P < 0.05 for Student's 2-tailed t-test.

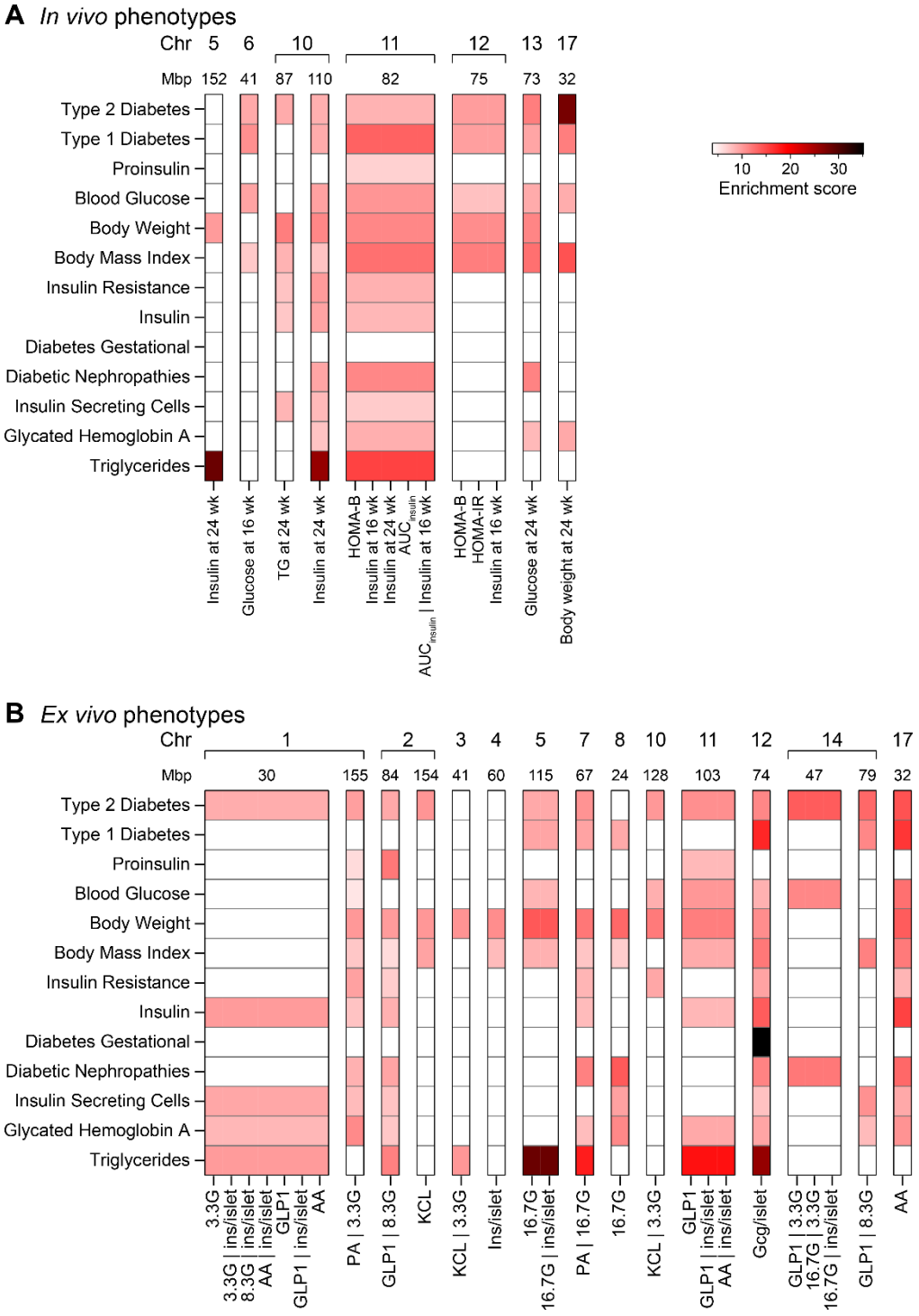

Figure S7. Diabetes GWAS enrichment at specific QTL.
Enrichment of specific GWAS traits at QTL identified from *in vivo* whole-body physiological phenotypes (**A**) and islet-based *ex vivo* phenotypes (**B**). Chromosome number and genomic position (Mbp) are shown for each QTL. Phenotypes measured in the mice are listed along the bottom. For each QTL, an enrichment score was computed for each GWAS trait (see **Methods**). Black corresponds to the highest score.

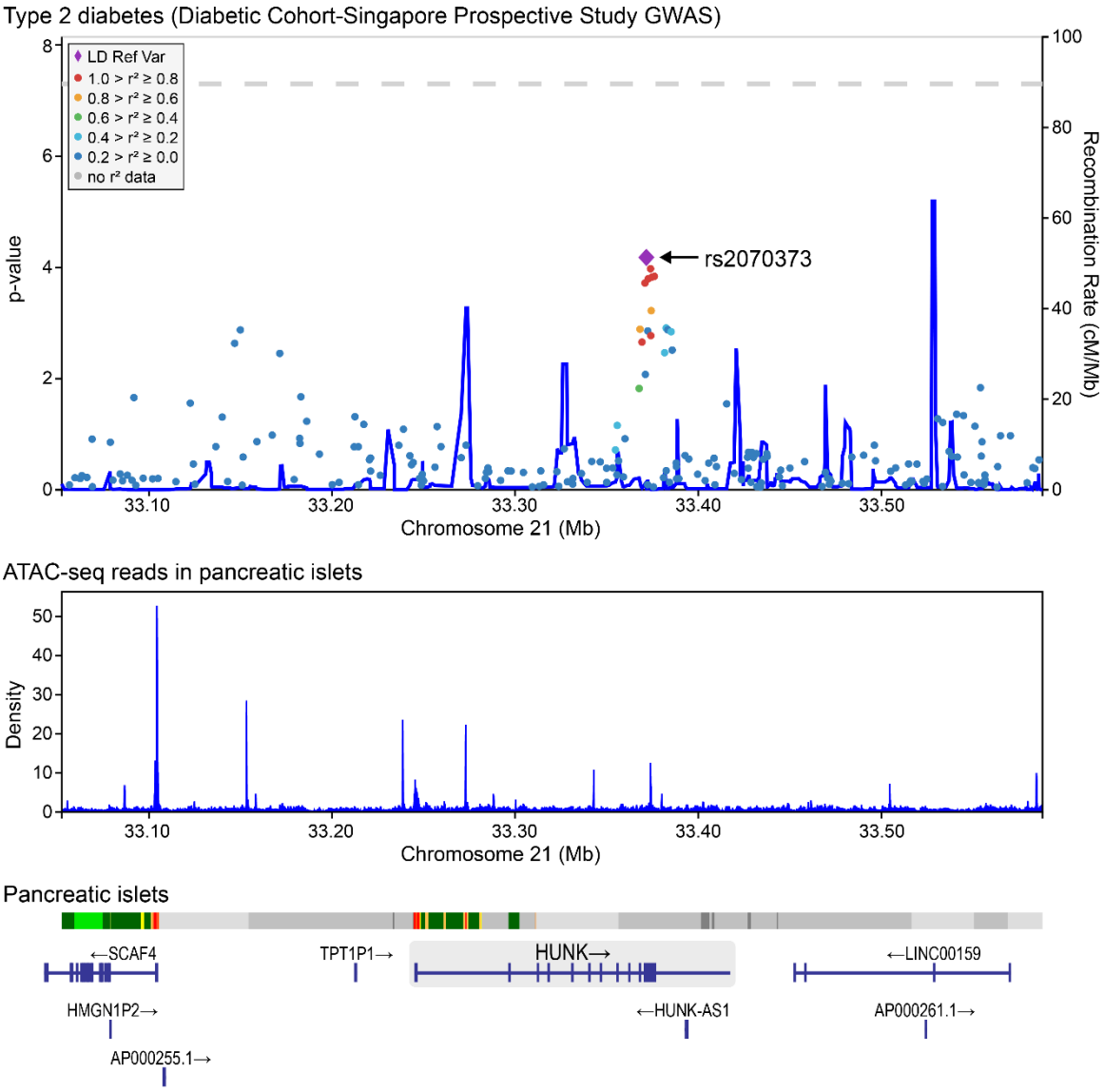

Figure S8. Type 2 Diabetes GWAS regional association plot for *HUNK*.
Regional association plot at the *HUNK* locus for type 2 diabetes in multi-ethnic cohorts from Southeast Asia (1). Data is available at the Type 2 Diabetes Knowledge Portal; http://www.type2diabetesgenetics.org/gene/geneInfo/HUNK.

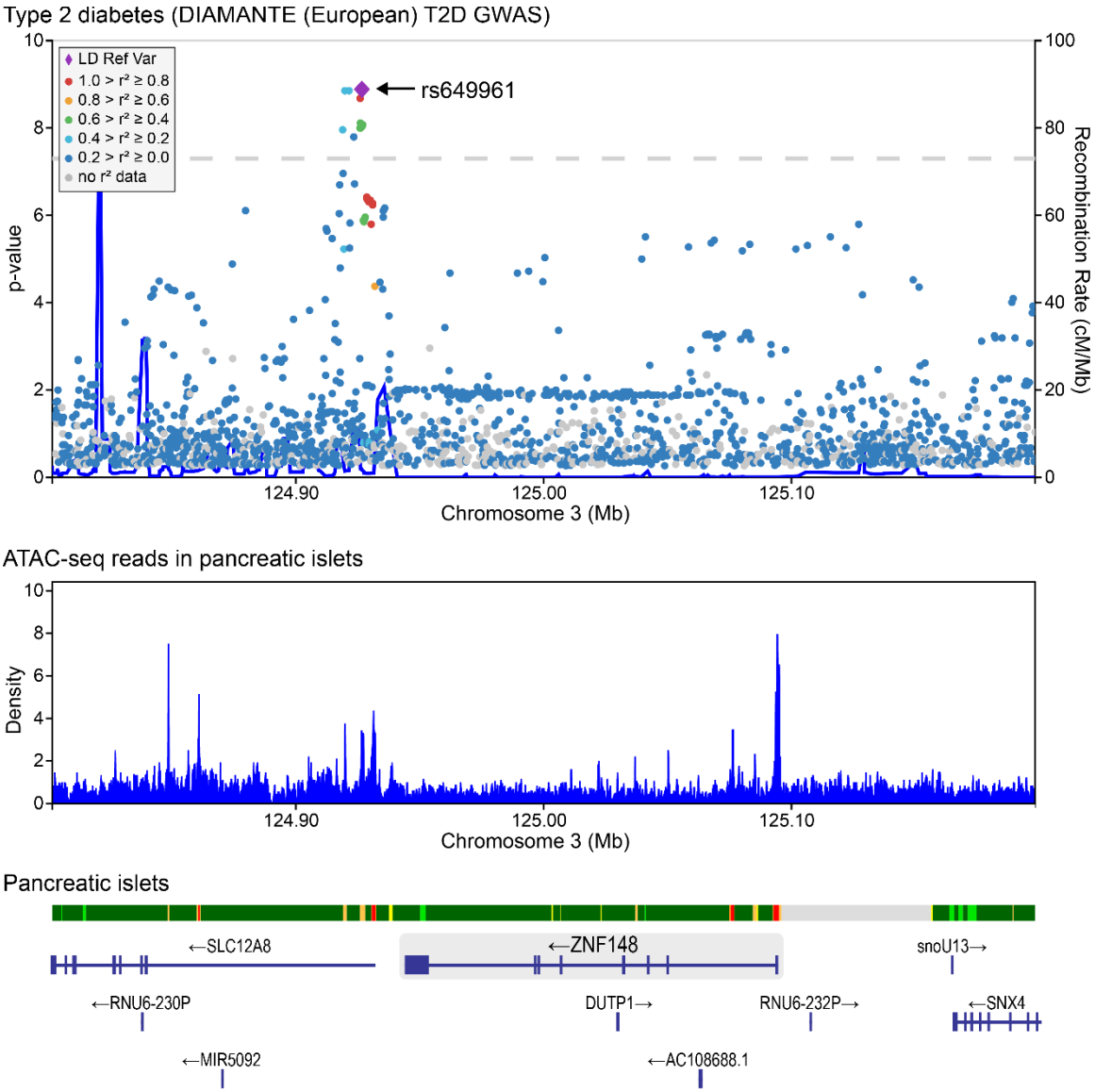

Figure S9. Type 2 Diabetes GWAS regional association plot for *ZNF148*.
Regional association plot at the *ZNF148* locus for the DIAMANTE (European) meta-analysis of type 2 diabetes (2). Data is available at the Type 2 Diabetes Knowledge Portal; http://www.type2diabetesgenetics.org/gene/geneInfo/ZNF148.

Supplementary tables

Table S1. QTL for islet-based *ex vivo* phenotypes and *in vivo* whole-body physiological phenotypes.

QTL identified for *ex vivo* islet-based studies (Tab 1). QTL identified for *in vivo* whole-body physiological phenotypes (Tab 2). Based on co-mapping and matched allele effect patterns (blue = low allele, orange = high allele), 30 and 19 QTL were identified for the *ex vivo* and *in vivo* phenotypes, respectively. SNP association profiles were determined for each phenotype, and used to identify syntenic regions enriched for diabetes-associated SNPs identified in human GWAS (see **Methods**).

Table S2. Candidate mediators for insulin secretion QTL.

List of mediator candidates identified at insulin secretion QTL on chromosomes 1, 3, 8, 11 and 19. Allele effect pattern for the mediator's local-eQTL (blue = low allele, orange = high allele), and the correlation between the expression of each mediator and the *ex vivo* islet traits (insulin secretion, glucagon secretion, number of islets per mouse, and the islet contents for insulin and glucagon), and the *in vivo* physiological traits are shown and color-coded; red for negative correlation, green for positive correlation.

Table S3. Primer sequences used for genotyping transgenic mice for *Ptpn18*, *Hunk* and *Zfp148*.

Table S4. Phenotype ontology terms used to link mouse and human traits.

Mouse traits were manually evaluated for the most appropriate Mammalian Phenotype Ontology (MPO) terms, which were then mapped to Human Phenotype Ontology (HPO) terms using PhenoHM. Asterisks identify the human terms that were manually assigned due to either an absence of mappings from the respective mouse terms, or an insufficient level of detail provided by the mapped human terms. AUC, area under the curve; wk, week; HOMA, homeostatic model assessment; IR, insulin resistance; B, beta-cell; oGTT, oral glucose tolerance test.

Table S5. Diabetes-related SNPs downloaded from GWAS Central.

List of 12,829 unique SNPs associated with diabetes-related phenotypes determined in humans. Chromosome (chr), position in base pair, marker id and trait are shown for each SNP.

Description of Hunk, Zfp148 and Ptpn18 transgenic mice.

Frozen embryos of *Hunk*^{KO} mice were provided by Dr. Vladimir Buchman, Molecular and Cellular Biology School of Biosciences, Cardiff University. *Hunk*-deficient mice were generated by targeting exon 4 of the *Hunk* gene for deletion (1). Exon 4 encodes amino acids 204 – 249 of the mature Hunk protein, which contains a portion of the Hunk protein kinase catalytic domain, including the conserved MgATP-coordinating Asp^{204}; subdomains VIII and IX. Further, deletion of exon 4 resulted in a frameshift upon joining exons 3 and 5, leading to a catalytically dead, truncated protein of 203 amino acids out of 714 amino acids in the full-length Hunk protein. To remove non-B6 alleles, founder transgenic mice were backcrossed 6 generations to C57BL/6J. Embryos for *Hunk*^{KO} mice were thawed and implanted into the uterus of pseudopregnant C57BL/6J female mice at the Transgenic Animal Facility at the University of Wisconsin. A conditional allele for *Zfp148* (*Zfp148*$^{flox/flox}$) was provided by Dr. Juanita Merchant, University of Arizona. *Zfp148*$^{flox/flox}$ mice were generated by introducing a *LoxP* site into intron 7, and a second *LoxP* site within the poly A termination signal located in exon 9, thereby targeting exons 8 and 9 for deletion when bred to a mouse expressing Cre-recombinase. Exons 8 and 9 encode the majority of the protein, and when deleted lead to mRNA instability and loss of Zfp148 protein (2). The *Zfp148*$^{flox/flox}$ mouse was originally generated in C57BL/6N-derived embryonic stem cells and maintained on C57BL/6N background (3). We bred these mice to C57BL/6J, and genotyped the progeny for the *Nnt* mutation (4), to obtain *Zfp148*$^{flox/flox}$ mice on a C57BL/6J background. We bred the *Zfp148*$^{flox/flox}$ mouse to B6(Cg)-Ins1tm1.1(cre)Thor/J mice (*Ins1*^{Cre}) developed by Thorens and colleagues, and is available at the Jackson Labs (stock no. 026801). This resulted in the specific deletion of *Zfp148* in β-cells (*β-Zfp148*^{KO}). CRISPR-mediated editing was used to mutate Asp^{197} to Ala^{197} in the *Ptpn18* gene product. A gRNA targeted to Asp^{197} (5'-ATATGTCCTGGCCAGACCAC-3') was *in vitro* transcribed (MEGAshortscript, ThermoFisher), and column-purified followed by ammonium acetate/ethanol precipitation (MEGAclear, ThermoFisher). Cas9 protein (40 ng/ul), gRNA (50 ng/ul), and single-stranded donor RNA (50

ng/ul) were microinjected into pro-nuclei of C57BL/6J mice. Upon weaning, genomic DNA was prepared from tail tissue samples, PCR amplified, uniquely indexed, pooled, and sequenced on a MiSeq 2x250 Nano flow cell. Founders were identified, backcrossed to C57BL/6J mice, and germline-transmitted F1's used to generate mice homozygous for the *Ptpn18*^{D197A} allele. Introduction of the D191A allele into the *Ptpn18* gene was verified by genome sequencing 110 bp upstream, and 190 bp downstream of the edit site; no other changes were detected. Further, the mutation creates an additional *Cac8I* restriction site, which was used to genotype offspring. A 366 bp fragment spanning the mutation yields two bands when digested with *Cac8I* (228 and 138 bp), whereas the mutation results in 3 bands (175, 137 and 53 bp).

Ex vivo insulin and glucagon secretion measurements.

Following digestion of the pancreas by collagenase (5), islets from each mouse were purified by hand-picking under a stereomicroscope and placed in recovery medium (RPMI, 11.1 mM glucose, antibiotics and 10% FBS) for 2 hours at 37˚C. Next, 50 similar-sized islets from each DO mouse were transferred to a 35 mm dish containing 3 ml Krebs Ringer Buffer (KRB: 118.41 mM NaCl, 4.69 mM KCl, 1.18 mM $MgSO_4$, 1.18 mM KH_2PO_4, 25 mM $NaHCO_3$, 5 mM HEPES, 2.52 mM $CaCl_2$, pH 7.4) containing 3 mM glucose, 0.5% BSA, and returned to 37˚C for an additional 45 minute pre-incubation period. Following the pre-incubation period, single islets were transferred to individual wells of a 96-well plate that contained 0.1 ml KRB plus one of the 7 secretion conditions: low (3.3 mM), medium (8.3 mM) or high (16.7 mM) glucose; low glucose plus KCl (40 mM); medium glucose plus a cocktail of 3 amino acids (AA; leucine, 0.5 mM; alanine, 1.25 mM; glutamine, 2 mM) or the incretin hormone GLP1 (100 nM); and high glucose plus palmitic acid (PA; 0.5 mM conjugated to 0.67% BSA). From each mouse, 6 individual islets were used per secretion condition, alternating the transfer between all 7 incubation conditions, to ensure similar sized islets were distributed between all conditions. The 96-well plate was returned to the 37˚C incubator for 45 mins, after which the media was transferred from each well to a 96-

well polypropylene plate, capped and frozen at -20˚C until insulin and glucagon was determined by RIA (insulin and glucagon secretion in response to 3.3 mM glucose) or ELISA (for all other secretion conditions). Three average-sized islets from each mouse were placed in 1 ml acid-EtOH and used to measure insulin and glucagon content by RIA. For insulin secretion, the geometric mean of the 6 individual islets/condition was computed and used for all subsequent analyses. For glucagon secretion, media that remained from the 6 wells that were stimulated with KCl + 3.3 mM glucose was pooled for each mouse and used for the glucagon measurement, yielding a single value per mouse. For each wave of 100 DO mice, 4 mice per day of the same sex were screened, alternating between females and males, until all 100 mice were surveyed, ~5 weeks.

Ontology-driven mapping of mouse traits to human traits.

The Mammalian Phenotype Ontology (MPO) and Human Phenotype Ontology (HPO) provides an unambiguous means for defining and comparing phenotypes across mice and humans, respectively. We evaluated our list of 32 diabetes-related *in vivo* and *ex vivo* mouse traits measured in mice, against the MPO, and selected the most appropriate MPO term to describe each trait, resulting in a set of 11 unique MPO phenotypes. For each mouse phenotype we identified an equivalent human phenotype, using the MPO-to-HPO mappings that we accessed from the human–mouse orthologous phenotype server, PhenoHM (6) (**Table S4**). In order to obtain a list of human traits that could be used to extract SNPs from GWAS Central (see below), we used the Unified Medical Language System to map the HPO terms to Medical Subject Headings (MeSH) terms. Finally, we included relevant disease terms for which there are no equivalent mouse trait, for example, “Type 1 Diabetes” and “Metabolic Syndrome”, to obtain a set of 16 MeSH-coded human diabetes-related traits.

Extracting diabetes-related SNPs from human GWAS.

GWAS Central is a comprehensive summary-level GWAS database that does not restrict its content to marker signals that exceed predefined P-value thresholds. The phenotype content of studies is manually evaluated and appropriate terms from the MeSH-controlled vocabulary are applied to standardize the phenotype descriptions.

1. Reed KR, Korobko IV, Ninkina N, Korobko EV, Hopkins BR, Platt JL, et al. Hunk/Mak-v is a negative regulator of intestinal cell proliferation. *BMC Cancer.* 2015;15:110.
2. Takeuchi A, Mishina Y, Miyaishi O, Kojima E, Hasegawa T, and Isobe K. Heterozygosity with respect to Zfp148 causes complete loss of fetal germ cells during mouse embryogenesis. *Nat Genet.* 2003;33(2):172-6.
3. Essien BE, Grasberger H, Romain RD, Law DJ, Veniaminova NA, Saqui-Salces M, et al. ZBP-89 regulates expression of tryptophan hydroxylase I and mucosal defense against Salmonella typhimurium in mice. *Gastroenterology.* 2013;144(7):1466-77, 77 e1-9.
4. Freeman H, Shimomura K, Horner E, Cox RD, and Ashcroft FM. Nicotinamide nucleotide transhydrogenase: a key role in insulin secretion. *Cell Metab.* 2006;3(1):35-45.
5. Rabaglia ME, Gray-Keller MP, Frey BL, Shortreed MR, Smith LM, and Attie AD. Alpha-Ketoisocaproate-induced hypersecretion of insulin by islets from diabetes-susceptible mice. *Am J Physiol Endocrinol Metab.* 2005;289(2):E218-24.
6. Sardana D, Vasa S, Vepachedu N, Chen J, Gudivada RC, Aronow BJ, et al. PhenoHM: human-mouse comparative phenome-genome server. *Nucleic acids research.* 2010;38(Web Server issue):W165-74.